iScience

CellPress
OPEN ACCESS

Article

Caenorhabditis elegans algn-2 Is Critical for Longevity Conferred by Enhanced Nonsense-Mediated mRNA Decay

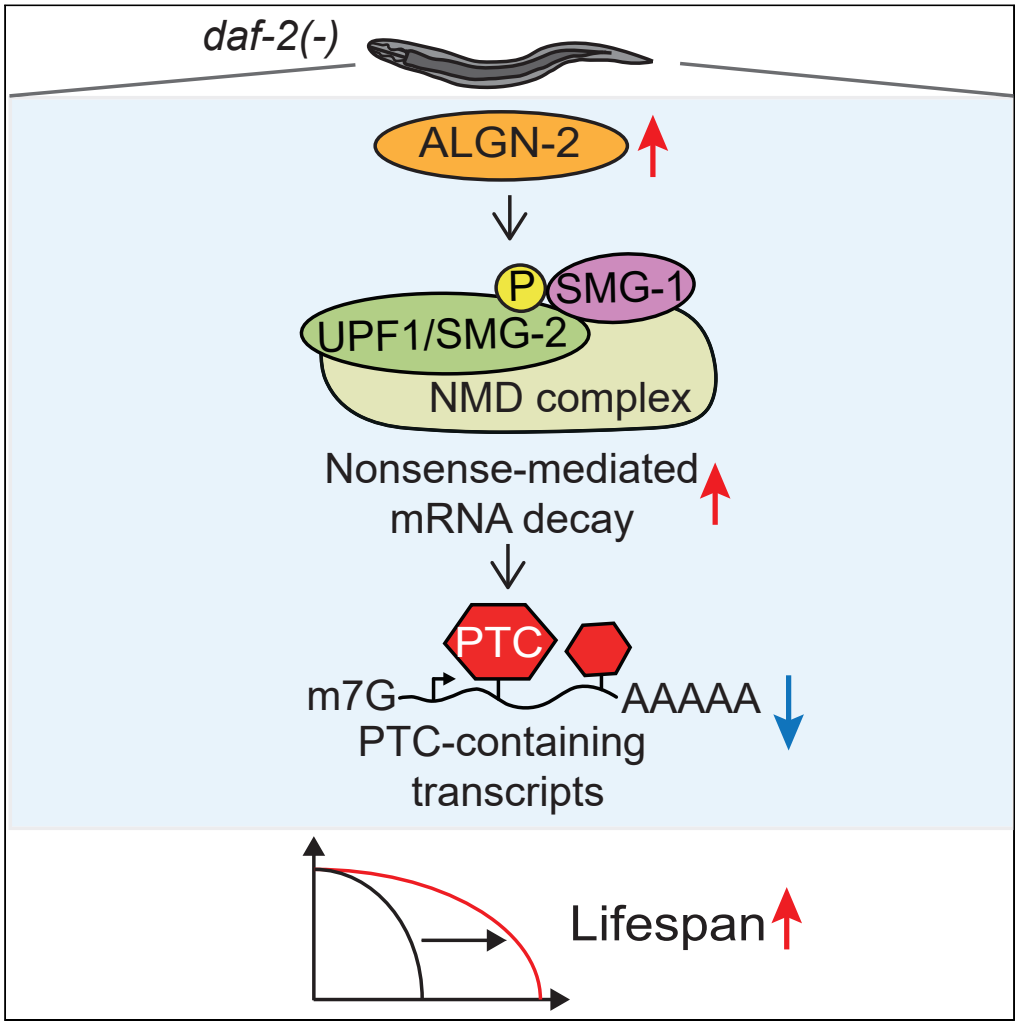

Eun Ji E. Kim,
Heehwa G. Son,
Hae-Eun H. Park,
Yoonji Jung,
Sujeong Kwon,
Seung-Jae V. Lee

seungjaevlee@kaist.ac.kr

HIGHLIGHTS

C. elegans algn-2 is a positive regulator of nonsense-mediated mRNA decay (NMD)

algn-2 is downregulated during aging and contributes to maintaining normal lifespan

algn-2 is required for longevity caused by various genetic interventions

Upregulation of ALGN-2 by inhibition of *daf-2* promotes longevity via increasing NMD

Kim et al., iScience *23*, 101713
November 20, 2020
https://doi.org/10.1016/j.isci.2020.101713

iScience

CellPress
OPEN ACCESS

Article

Caenorhabditis elegans algn-2 Is Critical for Longevity Conferred by Enhanced Nonsense-Mediated mRNA Decay

Eun Ji E. Kim,[1] Heehwa G. Son,[1] Hae-Eun H. Park,[1] Yoonji Jung,[1] Sujeong Kwon,[1] and Seung-Jae V. Lee[1,2,*]

SUMMARY

Nonsense-mediated mRNA decay (NMD) is a biological surveillance mechanism that eliminates mRNA transcripts with premature termination codons. In *Caenorhabditis elegans*, NMD contributes to longevity by enhancing RNA quality. Here, we aimed at identifying NMD-modulating factors that are crucial for longevity in *C. elegans* by performing genetic screens. We showed that knocking down each of *algn-2*/asparagine-linked glycosylation protein, *zip-1*/bZIP transcription factor, and *C44B11.1*/FAS apoptotic inhibitory molecule increased the transcript levels of NMD targets. Among these, *algn-2* exhibited an age-dependent decrease in its expression and was required for maintaining normal lifespan and for longevity caused by various genetic interventions. We further demonstrated that upregulation of ALGN-2 by inhibition of *daf-2*/insulin/IGF-1 receptor contributed to longevity in an NMD-dependent manner. Thus, *algn-2*, a positive regulator of NMD, plays a crucial role in longevity in *C. elegans*, likely by enhancing RNA surveillance. Our study will help understand how NMD-mediated mRNA quality control extends animal lifespan.

INTRODUCTION

Eukaryotic cells are equipped with mechanisms that maintain proper gene expression and prevent the production of deleterious proteins. Nonsense-mediated mRNA decay (NMD) is an mRNA quality control mechanism that monitors and degrades abnormal transcripts with premature termination codons (PTCs) (He and Jacobson, 2015; Kim and Maquat, 2019; Kurosaki et al., 2019). NMD targets also include mRNAs with long (>1 kb) 3′ untranslated regions, upstream open reading frames, or selenocysteine-encoding UGA codons (He and Jacobson, 2015; Kim and Maquat, 2019; Kurosaki et al., 2019). Thus, NMD is crucial for RNA quality surveillance and the maintenance of the correct transcriptome in organisms.

Key evolutionarily conserved components of NMD have been identified by using model organisms, including the budding yeast *Saccharomyces cerevisiae* and the nematode *Caenorhabditis elegans*. A genetic screen using *C. elegans* has identified the main NMD components, *smg* (*suppressor with morphological effect on genitalia*)*-1* through *smg-7* (Hodgkin et al., 1989; Mango, 2001). SMG-1 is a phosphatidylinositol 3-kinase-related kinase that phosphorylates SMG-2/UPF1 RNA helicase (Hodgkin et al., 1989; Mango, 2001). This event activates the NMD machinery and leads to the cleavage of target mRNAs via the endonuclease SMG-6 (Eberle et al., 2009; Huntzinger et al., 2008; Lykke-Andersen et al., 2014). Subsequently, the target mRNAs are degraded by exosomes and exonucleases (Schmid and Jensen, 2008). Additional research has led to the discovery of other NMD components, including *smg-8*, *smg-9*, *smgl* (*smg lethal*)*-1*, and *smgl-2* (Longman et al., 2007; Yamashita et al., 2009); however, the role of *smg-8* in NMD has been challenged by the characterization of *smg-8* mutants (Rosains and Mango, 2012). Unlike the abovementioned, extensively characterized NMD components, the upstream regulators of NMD remain underexplored.

In *C. elegans*, NMD contributes to longevity by influencing the levels of various mRNAs (Son et al., 2017). Specifically, NMD function is crucial for extended lifespan conferred by reduced insulin/IGF-1 signaling (IIS), an evolutionarily conserved aging-regulatory pathway. Reduced IIS increases NMD and subsequently decreases the levels of specific transcripts, including *yars-2b.1*/tyrosyl-tRNA synthetase isoform b.1, and this, in turn, contributes to longevity. In addition, NMD is upregulated to modulate the splicing of various

[1]Department of Biological Sciences, Korea Advanced Institute of Science and Technology, 291 Daehak-ro, Yuseong-gu, Daejeon 34141, South Korea

[2]Lead Contact

*Correspondence: seungjaevlee@kaist.ac.kr

https://doi.org/10.1016/j.isci.2020.101713

gene transcripts that are important for dietary restriction-induced longevity (Tabrez et al., 2017). Despite these initial findings on the roles of the known NMD components in longevity in *C. elegans*, it remains poorly understood whether and how NMD contributes to extended lifespan and delayed aging.

In the present report, we identified modulators of NMD by employing two genetic screens. We first performed a genome-wide RNAi screen for the modifiers of NMD by using a fluorescent NMD reporter and subsequently validated the results by measuring the level of *rpl-7A*, an endogenous NMD target transcript. We found that RNAi targeting each of *algn-2*/asparagine-linked glycosylation protein, *zip-1*/bZIP transcription factor, and *C44B11.1*/FAS apoptotic inhibitory molecule (FAIM) increased the levels of the *rpl-7A* transcript. We also showed that two of the mutants isolated from our mutagenesis screen exhibited decreased *rpl-7A* transcript levels. We then found that *algn-2,* the expression of which declined during aging, was required for maintaining the normal lifespan. Furthermore, we showed that knocking down *algn-2* significantly decreased the longevity conferred by various genetic interventions, including *daf-2*/insulin/IGF-1 receptor mutations, dietary restriction mimetic *eat-2* mutations, and mitochondrial respiration-defective *isp-1* mutations. We further showed that ALGN-2 was upregulated upon the genetic inhibition of the *daf-2*/insulin/IGF-1 receptor and contributed to a long lifespan in an SMG-2-dependent manner. Overall, our study identified previously unknown modulators of NMD, including *algn-2*, which plays key roles in RNA quality control and organismal longevity.

RESULTS

A Genome-wide RNAi Screen Identified Modifiers of NMD

To identify NMD regulators, we first performed a genome-wide RNAi screen in a liquid culture system using an NMD-responsive GFP reporter (Figure 1A). The NMD reporter contains a PTC in the first exon of the GFP-fused *lacZ* gene, driven by a ubiquitous *sec-23* promoter, *sec-23p::gfp::lacZ(PTC)* (Longman et al., 2007) (Figure 1A). Under normal conditions, this transcript is degraded by NMD, and the worms, therefore, display dim GFP fluorescence (Figure 1A). We used a sensitized loss-of-function mutant background of *smg-1*, which encodes a kinase that phosphorylates SMG-2/UPF1 and induces NMD (Grimson et al., 2004). With the increased basal GFP expression of the reporter in the *smg-1(−)* mutant background, we searched for genes whose knockdown further changed the green fluorescence intensity (Figure 1A). We initially found that the GFP expression levels were further increased by 39 RNAi clones and decreased by 38 RNAi clones (arbitrary cutoff: > 1.5 and −1.5 <, Figure 1B and Table S1). By repeating the experiments six times, we confirmed that 25 and 7 RNAi clones increased and decreased the GFP levels, respectively (cutoff of mean value: > 0.6 and −0.6 <, Figure 1C and Table S1).

RNAi Targeting *algn-2*, *zip-1*, or *C44B11.1* Increased the Level of an NMD Target Transcript, *rpl-7A(PTC)*

We then validated the RNAi clones from our liquid culture-based screen by using a solid-medium culture system. We found that 24 of the 25 RNAi clones that increased the GFP levels in liquid culture did the same on solid media (Figures 2A and 2B, Table S1). However, none of the seven RNAi clones that decreased the GFP levels in liquid culture did on solid media (Figures S1A and S1B, Table S1). We further determined the effects of our hit RNAi clones on an endogenous NMD target gene, *rpl-7A(PTC)* (Mitrovich and Anderson, 2000) (Figure 2C and Table S1). We found that RNAi knockdown of *algn-2*, *zip-1*, or *C44B11.1* significantly increased the level of the *rpl-7A(PTC)* transcript in *smg-1(−)* mutants as well as in wild-type animals (Figures 2D–2G, Table S1). Thus, *algn-2*, *zip-1*, and *C44B11.1* appear to be positive modulators of NMD.

An EMS Mutagenesis Screen Identified Potential Negative Modulators of NMD

Because we were not able to identify RNAi clones that reliably decreased the NMD reporter GFP level from our genome-wide RNAi screen (Figure S1), we sought to identify such genetic inhibition by employing an EMS mutagenesis screen (Figure S3A). From the 83,400 mutagenized haploid genomes of *smg-1(−); sec-23p::gfp::lacZ(PTC)* animals, we obtained 11 and 9 fertile mutant strains with decreased and increased GFP levels, respectively (Figure S3A). We then confirmed the reproducibility of the results by quantifying the fluorescence levels of the mutants (Figure S3B). Because of the absence of screened RNAi clones that reproducibly decreased the NMD reporter GFP level, we focused on potential negative NMD regulator mutants. Among the 11 mutants that displayed reduced NMD reporter GFP levels, we found that two mutant alleles, *yh47* and *yh57*, significantly decreased the level of the *rpl-7A(PTC)* transcript using qRT-

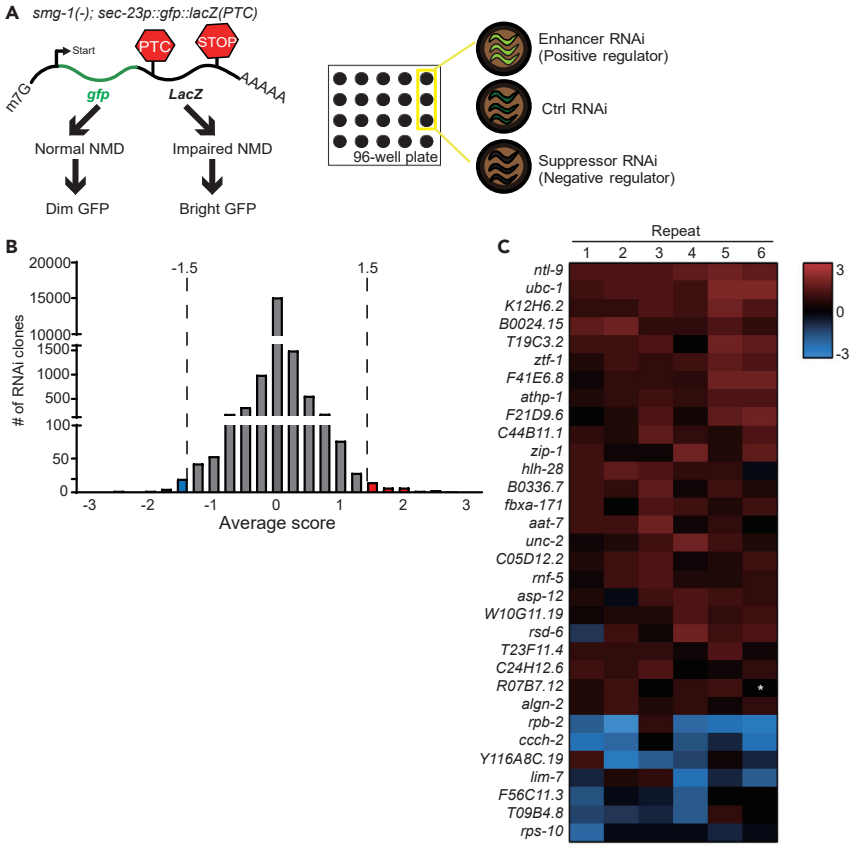

Figure 1. A Genome-wide RNAi Screen for NMD Modulators

(A) Schematic showing a PTC-bearing *gfp-lacZ* transgene in a *smg-1(tm849)* [*smg-1(−)*] mutant background [*smg-1(−); sec-23p::gfp::lacZ(PTC)*], which was used as a reporter for a genome-wide RNAi screen in a liquid culture system (score range: −3 to +3). *gfp* RNAi and control RNAi (Ctrl) were used as controls to provide references for scores −3 and 0, respectively.

(B) Summary of initial genome-wide RNAi screen data (arbitrary cutoff scores: < −1.5 and >1.5).

(C) The assay was repeated for RNAi clones that passed the cutoff of the initial screen six times, and the average scores from the six experiments were used to narrow down the candidates (mean cutoff scores: < −0.6 and >0.6). Twenty-five and seven RNAi clones increased and decreased the GFP level of the reporter, respectively. Asterisk (*) indicates lack of data because worms were not placed in the designated well. See Table S1 for the descriptions and scores of indicated RNAi clones from the screen.

PCR (Figure S3C). These data suggest that genes that are mutated by *yh47* and *yh57* alleles encode potential negative regulators of NMD.

algn-2 Whose mRNA Level Decreases with Age Is Required for Maintaining the Normal Lifespan

We previously reported that NMD function decreases with age and mediates longevity conferred by reduced IIS in *C. elegans* (Son et al., 2017). Thus, in the present study, we tested whether *algn-2*, *zip-1*, or *C44B11.1* exhibited age-dependent expression changes or contributed to longevity. We found that the mRNA levels of *algn-2* and *zip-1* decreased with age, whereas that of *C44B11.1* exhibited an age-dependent increase (Figures 3A–3C). These data imply a functional association between *algn-2*, *zip-1*, or *C44B11.1* and aging in *C. elegans*. We then determined whether RNAi targeting each of *algn-2*, *zip-1*, and *C44B11.1* affected lifespan. We found that *algn-2* RNAi significantly shortened the lifespan of wild-type animals, whereas *zip-1* RNAi or *C44B11.1* RNAi did not (Figures 3D–3F). Thus, *algn-2*, which exhibits an age-dependent decrease in mRNA levels, is required for the maintenance of the normal lifespan.

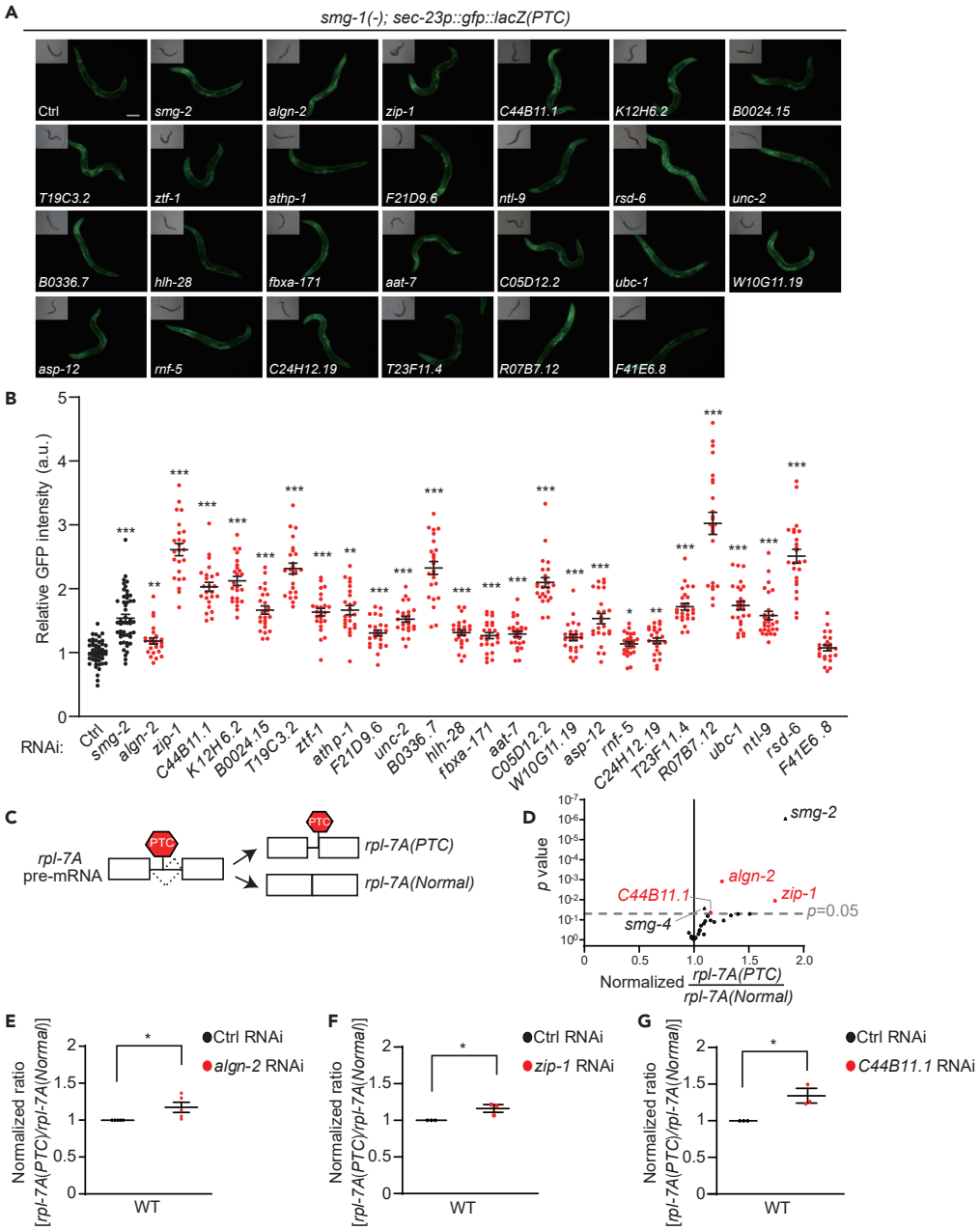

Figure 2. Validation of NMD Modulators Identified from Genome-wide RNAi Screen

(A) Representative RNAi clones targeting potential NMD regulators on solid media. Of 25 potential positive NMD regulators identified from the genome-wide RNAi screen, 24 increased the GFP expression level on solid culture media (scale bar, 100 μm). Ctrl, control RNAi. *smg-2* RNAi was used as a positive control.

(B) Quantification data for panel (A). Error bars represent SEM (two-tailed Student's t test, *p < 0.05, **p < 0.01, ***p < 0.001, n ≥ 24 from three independent experiments). See Table S1 for the relative GFP level change caused by treating with each RNAi clone.

(C) Schematic diagram showing the alternative splicing of *rpl-7A* that generates *rpl-7A(Normal)*, a normal transcript, and *rpl-7A(PTC)*, an established NMD target transcript.

(D) Volcano plot showing normalized *rpl-7A(PTC)* level and p values from RT-PCR in *smg-1(tm849)* mutants with each of the RNAi clones. p values were calculated using a two-tailed Student's t test. A dotted line indicates p = 0.05, and black triangles indicate *smg-2* RNAi and *smg-4* RNAi, which were used as positive controls. See Table S1 for the normalized *rpl-7A(PTC)* ratio for the indicated RNAi clones and Figure S1 legends for discussion regarding (B and D).

Figure 2. *Continued*
(E–G) Normalized *rpl-7A(PTC)* level obtained from qRT-PCR in wild-type (WT) worms treated with *algn-2* RNAi (n = 5) (E), *zip-1* RNAi (n = 3) (F), and *C44B11.1* RNAi (n = 3) (G). Error bars represent SEM (two-tailed Student's t test, *p < 0.05).

algn-2 Is Crucial for Longevity Conferred by Various Interventions, including *daf-2*/Insulin/IGF-1 Receptor Mutations that Enhance NMD

Next, we focused our functional analysis on the role of *algn-2* in the lifespan. We showed that *algn-2* RNAi did not further decrease short lifespan caused by mutations in *smg-2* (Figure 4A). Thus, *algn-2* appears to act together with SMG-2 to maintain normal lifespan in *C. elegans*. We have previously reported that SMG-2, an RNA helicase essential for NMD (Kim and Maquat, 2019; Page et al., 1999), is critical for *C. elegans* longevity resulting from reduced IIS, which increases NMD (Son et al., 2017). We therefore tested whether *algn-2* contributed to the longevity conferred by reduced IIS. We found that *algn-2* RNAi significantly decreased the long lifespan conferred by two mutant alleles of *daf-2*/insulin/IGF-1 receptor gene, *e1370* and *e1368* (Figures 4B and 4C), or a phosphoinositide-3 kinase gene mutation, *age-1(hx546)* (Figure 4D). In addition, *algn-2* RNAi did not further decrease the shortened lifespan of *smg-2(−); daf-2(−)* mutants (Figure 4E). These results suggest that *algn-2* contributes to longevity conferred by reduced insulin/IGF-1 signaling by acting together with SMG-2.

We also tested the effect of *algn-2* RNAi on the longevity of dietary restriction mimetic *eat-2(−)* mutants and mitochondrial respiration-defective *isp-1(−)* mutants. We found that RNAi knockdown of *algn-2* significantly shortened the long lifespan of *eat-2(−)* mutants (Figure 4F) and *isp-1(−)* mutants (Figure 4G). These data indicate that *algn-2* is generally required for lifespan extension caused by various interventions in *C. elegans*.

Genetic Inhibition of *daf-2* Upregulates ALGN-2 to Increase NMD Function and Lifespan

We next generated transgenic animals expressing GFP-fused ALGN-2 under the promoter of *algn-2* (*algn-2p::algn-2::gfp*) and detected ALGN-2::GFP in the intestine and neurons (Figure 5A). We showed that ALGN-2::GFP was localized in the cytoplasm of the cells (Figure 5B), consistent with the localization of mammalian ALG2, the ALGN-2 ortholog, on the cytosolic face of the endoplasmic reticulum (ER) (Dean and Gao, 2014).

We then examined whether the genetic inhibition of *daf-2* affected the level of ALGN-2. Interestingly, *daf-2* RNAi significantly increased the level of ALGN-2::GFP (Figures 5C and 5D), without affecting that of *algn-2* mRNA (Figure S2B), suggesting that reduced insulin/IGF-1 signaling upregulates ALGN-2 at the post-transcriptional level. Next, we determined whether *algn-2* affected NMD function in *daf-2(−)* mutants. Specifically, we measured the level of *rpl-12(PTC)* transcript, an endogenous NMD target whose level decreases in *daf-2(−)* mutants and increases with age (Mitrovich and Anderson, 2000; Son et al., 2017) (Figure 5E). We showed that *algn-2* RNAi substantially increased the *rpl-12(PTC)* level in *daf-2(−)* mutants (Figure 5E). Together, these data suggest that upregulation of ALGN-2 conferred by reduced insulin/IGF-1 signaling enhances NMD in *C. elegans*.

Lastly, we tested whether the transgenic overexpression of *algn-2::gfp* affected lifespan. We found that the transgene that expressed *algn-2::gfp* at the highest level among three lines (Figures S5A and S5B) significantly increased lifespan (Figure 5F), whereas the other two did not (Figure S5C). Together, these data suggest that upregulation of ALGN-2 can increase lifespan by enhancing NMD.

DISCUSSION

ALGN-2, an NMD Modulator, Contributes to Longevity in *C. elegans*

NMD is an evolutionarily conserved process that is crucial for the monitoring and maintenance of RNA quality and, therefore, cellular RNA homeostasis. In the present report, we performed a series of genetic screens to identify modifiers of NMD. From our genome-wide RNAi screen, we identified *algn-2*, *zip-1*, and *C44B11.1*/FAIM as NMD modulators that were required for downregulation of NMD target transcripts. Among these, we showed that *algn-2* contributed to longevity conferred by *daf-2*/insulin/IGF-1 receptor mutations in an NMD-dependent manner. Our study highlights the power of genetic screens for identifying factors that regulate NMD function and thereby affect organismal lifespan, possibly through the maintenance of RNA quality.

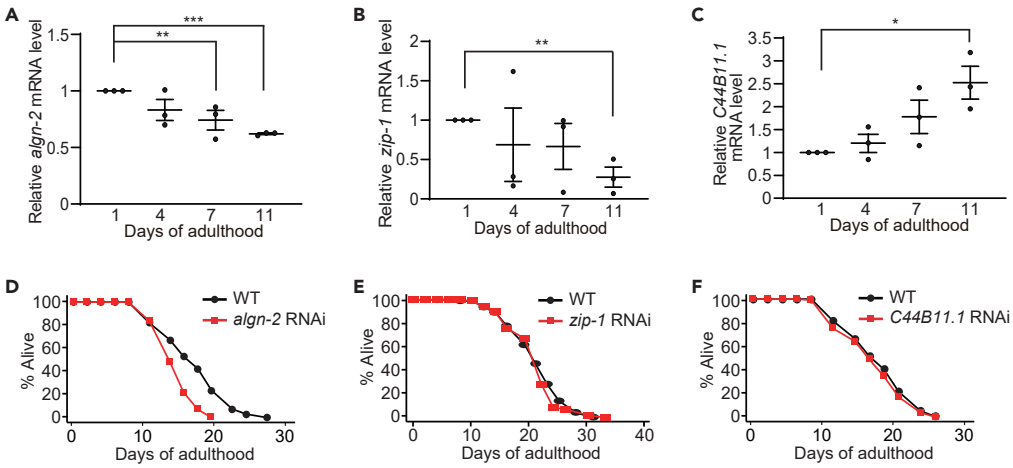

Figure 3. Age-Dependent Expression Changes in *algn-2*, *zip-1*, and *C44B11.1*, and Their Functions in Lifespan

(A–C) mRNA levels of *algn-2* (A), *zip-1* (B), and *C44B11.1* (C) in day 1, 4, 7, and 11 adult wild-type worms analyzed by using qRT-PCR (n = 3). Error bars represent SEM (two-tailed Student's t test, *p < 0.05, **p < 0.01, ***p < 0.001). See Figure S4 legends for discussion regarding the expression changes in *C44B11.1*.

(D–F) RNAi targeting *algn-2* significantly reduced the lifespan of wild-type (WT) animals (D), but RNAi targeting *zip-1* (E) or *C44B11.1* (F) did not. *algn-2* RNAi, *zip-1* RNAi, and *C44B11.1* RNAi significantly decreased the mRNA levels of *algn-2*, *zip-1*, and *C44B11.1*, respectively (Figures S2A, S2C, and S2D). See Table S3 for statistical analysis and additional lifespan data.

ALGN-2 May Affect NMD Function by Regulating the ER Stress Response

ALG2, the mammalian ortholog of ALGN-2, is a mannosyltransferase located at the ER membrane (Dean and Gao, 2014). ALG2 catalyzes the second and third mannosylation steps, which convert guanosine diphosphate mannose to core asparagine (N)-glycan (Li et al., 2019). Immature glycosylation causes severe ER stress, resulting in the activation of the unfolded protein response (UPR) (Cherepanova et al., 2016). ER stress can inhibit NMD and causes the NMD complex to be localized to the ER (Sakaki et al., 2012; Usuki et al., 2019). *algn-2* RNAi also increases ER stress in *C. elegans* (Akiyoshi et al., 2015; Ho et al., 2019) and may therefore decrease NMD by altering ER stress responses. In addition, defects in N-linked glycosylation pathway genes, including *ALG2*, are linked to congenital myasthenic syndrome (CMS), which involves the impairment of signal transmission at neuromuscular synapses (Cossins et al., 2013; Engel, 2018). Interestingly, NMD is impaired in some types of CMS (Rahman and Nasrin, 2016), suggesting that ALG2-regulated NMD processes play a role in the pathophysiology of CMS. Further studies are required to dissect the mechanisms by which inhibition of *algn-2* affects the pathophysiology of the disease and NMD function potentially through affecting ER stress.

algn-2 Upregulates NMD in an SMG-2-Dependent Manner

One interesting aspect of our study is that we identified *algn-2* from an RNAi screen that used an NMD reporter in a *smg-1* mutant background. Interestingly, we found that *algn-2* RNAi did not affect the lifespan of *smg-2* mutants. Our previous report on NMD and longevity (Son et al., 2017) indicates that different SMG components differentially contribute to NMD function. Specifically, knockdown of *smg-1* has an intermediate effect on NMD function among five *smg* genes that we functionally tested. In contrast, *smg-2* RNAi has the biggest effect on NMD function. These data suggest that genetic inhibition of *smg-2* causes more severe impacts on NMD function than that of *smg-1* does. Thus, we speculate that *algn-2* RNAi did not further decrease the lifespan of *smg-2(−)* animals, while influencing NMD target levels in *smg-1(−)* mutants, because of their differential effects on NMD functions.

NMD-Regulated RNA Quality Control Is Crucial for Organismal Longevity

Recent reports indicate that NMD-mediated RNA homeostasis is critical for longevity in *C. elegans* (Son et al., 2017; Tabrez et al., 2017). These studies highlight the importance of NMD for clearing abnormal transcripts and promoting RNA homeostasis, which may help animals maintain health during aging. However, it remained unknown which factor causes a functional decline of NMD during aging. Our data suggest that

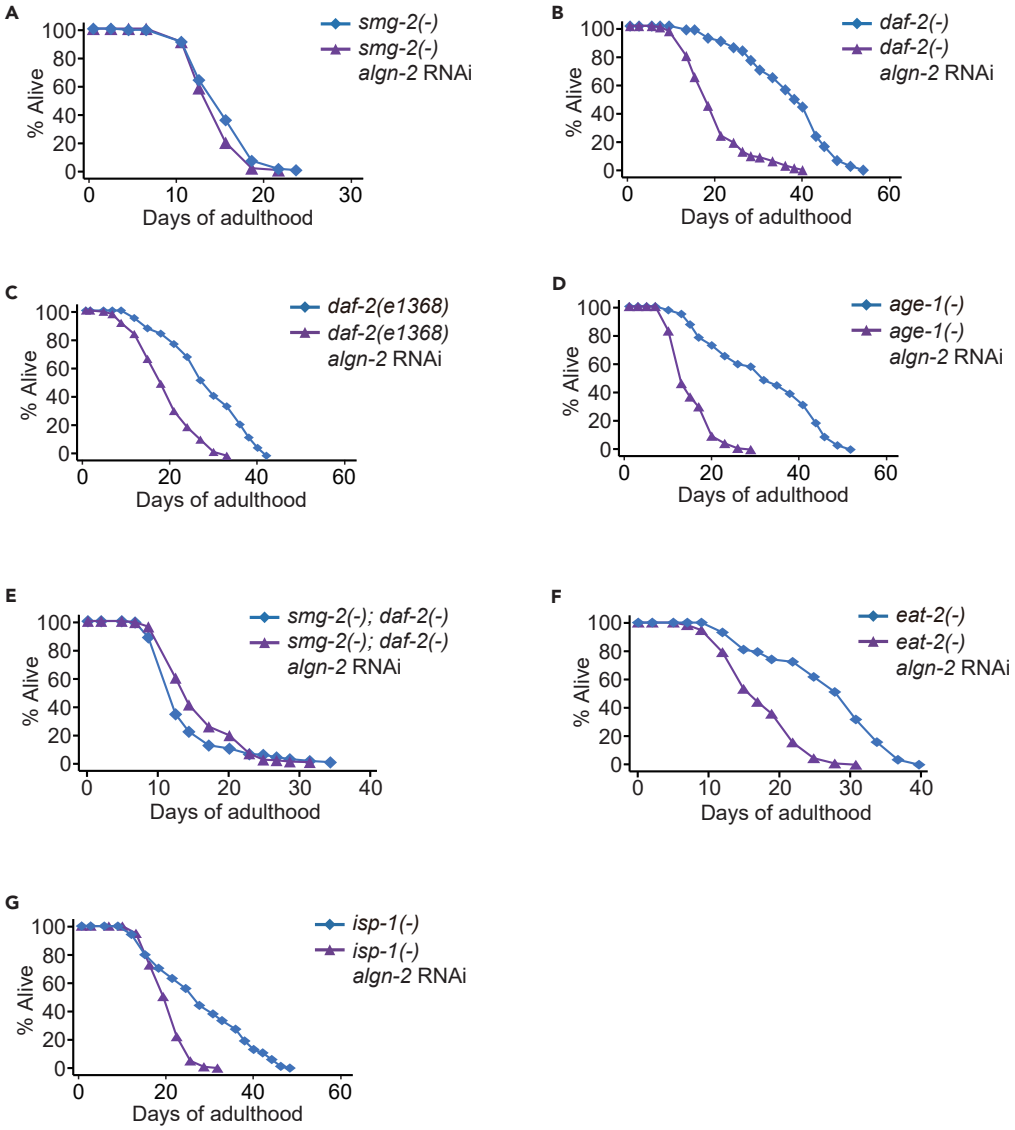

Figure 4. *algn-2* Contributes to Longevity Conferred by Various Interventions, including Reduced Insulin/IGF-1 Signaling by Acting Together with SMG-2

(A) *algn-2* RNAi did not decrease the lifespan of *smg-2(qd101)* [*smg-2(−)*] mutants.

(B–D) RNAi targeting *algn-2* significantly decreased the long lifespan of *daf-2(e1370)* [*daf-2(−)*] (B), *daf-2(e1368)* (C), and *age-1(hx546)* [*age-1(−)*] (D) mutants. Different from *algn-2* RNAi, neither *zip-1* RNAi nor *C44B11.1* affected the lifespan of *daf-2(−)* mutants (Figures S4A and S4B).

(E) *algn-2* RNAi had a small effect on the lifespan of *smg-2(−); daf-2(−)* double mutants. *algn-2* mRNA levels were not changed by *smg-2(−)* or *daf-2(−)* mutations (Figure S2B).

(F and G) *algn-2* RNAi shortened longevity induced by *eat-2(ad1116)* [*eat-2(−)*] (F) and *isp-1(qm150)* [*isp-1(−)*] (G) mutations. See Table S3 for statistical analysis and additional lifespan data.

reduced levels of factors that regulate NMD, including *algn-2*, underlie age-dependent decreases in NMD and possibly result in impaired RNA quality control. Our previous reports have also indicated that the NMD in the nervous system is crucial for lifespan extension (Son et al., 2017). Because the brain is the organ that expresses *Alg2* at the highest level in young mice (Imamura et al., 2014), *Alg2* expression in the brain may decrease in an age-dependent manner, perhaps contributing to the shortening of the lifespan by reducing NMD efficiency. It will be interesting to test whether preserving or increasing the levels of positive NMD modulators, including ALG2/ALGN-2, can be exploited as a strategy for avoiding the adverse effects of age-dependent declines in RNA quality, in particular in the nervous systems.

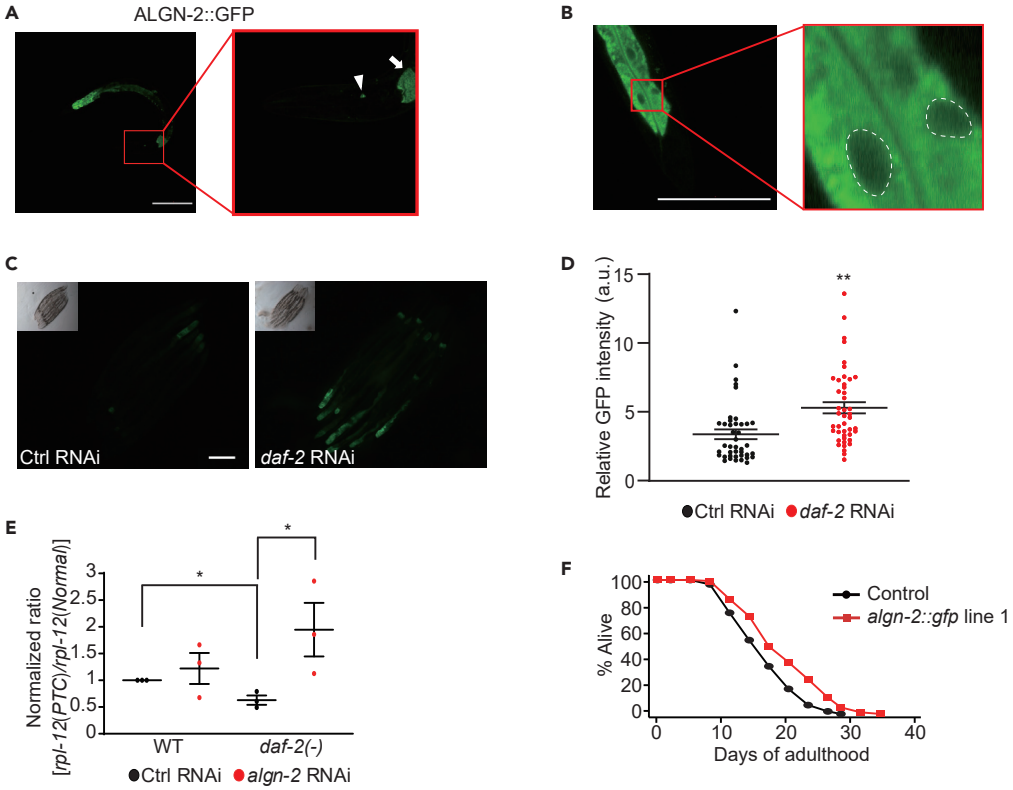

Figure 5. *algn-2* Is Upregulated by the Genetic Inhibition of *daf-2* for Enhancing NMD Function and Sufficient to Increase Lifespan

(A) Images of *algn-2::gfp*-expressing transgenic animals. The image in the red box focusing on the head region of the same worm on the left was obtained by using high magnification (scale bar, 100 μm) (arrow: intestine, arrowhead: neurons).

(B) The intestinal region of *algn-2::gfp*-expressing transgenic animals obtained by using a confocal microscope (scale bar, 100 μm). The image in the red box is enlarged from the indicated region on the left. Areas in white dashed lines indicate the nuclei.

(C) The images of *algn-2::gfp* worms treated with control (Ctrl) RNAi and *daf-2* RNAi (scale bar, 100 μm).

(D) Quantification of ALGN-2:GFP levels in (C). Error bars represent SEM (two-tailed Student's *t*-test, **$p < 0.01$, $n = 40$ from three independent experiments).

(E) The effect of *daf-2(−)* mutation and *algn-2* RNAi on the expression level of *rpl-12(PTC)* measured by using qRT-PCR ($n = 3$). Error bars represent SEM (two-tailed Student's t test, *$p < 0.05$).

(F) *algn-2::gfp* line 1 (*yhEx540[algn-2p::algn-2::gfp; ofm-1p::rfp]*) increased the lifespan of control (*ofm-1p::rfp*) worms. See Table S3 for statistical analysis and additional lifespan data.

Limitations of the Study

Although we identified *algn-2* as a positive regulator of NMD, which contributed to longevity in *C. elegans*, the biochemical mechanisms by which ALGN-2 affects NMD functions remain elusive. In addition, global transcriptomic analysis will help identify all the target transcripts of *algn-2*. Although we showed that decreased NMD function due to *smg-1(−)* was suppressed by *yh47* and *yh57*, two mutant alleles that we identified from our mutagenesis screen, the molecular identities of the mutations are unknown. Additionally, we did not test whether *algn-2* modulated NMD in a cell autonomous or a cell non-autonomous manner. These are important issues that need to be addressed in future studies.

Resource Availability

Lead Contact

Further request and information for resources and reagents used in this published article should be directed and will be fulfilled by the Lead Contact, Seung-Jae V. Lee (seungjaevlee@kaist.ac.kr).

Materials Availability

All data analyzed and generated in this research are included in this published article and supplemental information.

Data and Code Availability

The published article includes all data generated in this study.

METHODS

All methods can be found in the accompanying Transparent Methods supplemental file.

SUPPLEMENTAL INFORMATION

Supplemental Information can be found online at https://doi.org/10.1016/j.isci.2020.101713.

ACKNOWLEDGMENTS

We thank all Lee lab members for help and discussion. This study is supported by the Korean Government (MSICT) through the National Research Foundation (NRF) of South Korea (NRF-2019R1A3B2067745) to S-J.V.L.

AUTHOR CONTRIBUTIONS

E.J.E.K., H.G.S., H.-E.H.P, Y.J., S.K., and S.-J.V.L designed the experiments. E.J.E.K., H.G.S., H.-E.H.P, Y.J., and S.K. performed the experiments. E.J.E.K. and S.-J.V.L. analyzed the data. E.J.E.K. and S.-J.V.L. wrote the manuscript.

DECLARATION OF INTERESTS

The authors declare no competing interests.

Received: May 28, 2020
Revised: September 10, 2020
Accepted: October 16, 2020
Published: November 20, 2020

REFERENCES

Akiyoshi, S., Nomura, K.H., Dejima, K., Murata, D., Matsuda, A., Kanaki, N., Takaki, T., Mihara, H., Nagaishi, T., Furukawa, S., et al. (2015). RNAi screening of human glycogene orthologs in the nematode *Caenorhabditis elegans* and the construction of the *C. elegans* glycogene database. Glycobiology *25*, 8–20.

Cherepanova, N., Shrimal, S., and Gilmore, R. (2016). N-linked glycosylation and homeostasis of the endoplasmic reticulum. Curr. Opin. Cel. Biol. *41*, 57–65.

Cossins, J., Belaya, K., Hicks, D., Salih, M.A., Finlayson, S., Carboni, N., Liu, W.W., Maxwell, S., Zoltowska, K., Farsani, G.T., et al. (2013). Congenital myasthenic syndromes due to mutations in ALG2 and ALG14. Brain *136*, 944–956.

Dean, N., and Gao, X.-D. (2014). Heterodimeric Alg13/Alg14 UDP-GlcNAc transferase (ALG13,14). In Handbook of Glycosyltransferases and Related Genes, N. Taniguchi, K. Honke, M. Fukuda, H. Narimatsu, Y. Yamaguchi, and T. Angata, eds. (Springer Japan), pp. 1231–1238.

Eberle, A.B., Lykke-Andersen, S., Mühlemann, O., and Jensen, T.H. (2009). SMG6 promotes endonucleolytic cleavage of nonsense mRNA in human cells. Nat. Struct. Mol. Biol. *16*, 49–55.

Engel, A.G. (2018). Congenital myasthenic syndromes in 2018. Curr. Neurol. Neurosci. Rep. *18*, 46.

Grimson, A., O'Connor, S., Newman, C.L., and Anderson, P. (2004). SMG-1 is a phosphatidylinositol kinase-related protein kinase required for nonsense-mediated mRNA Decay in *Caenorhabditis elegans*. Mol. Cell. Biol. *24*, 7483–7490.

He, F., and Jacobson, A. (2015). Nonsense-mediated mRNA decay: degradation of defective transcripts is only part of the story. Annu. Rev. Genet. *49*, 339–366.

Ho, N., Wu, H., Xu, J., Koh, J.H., Yap, W.S., Goh, W.W.B., Chong, S.C., Taubert, S., and Thibault, G. (2019). ER stress sensor Ire1 deploys a divergent transcriptional program in response to lipid bilayer stress. bioRxiv, 774133.

Hodgkin, J., Papp, A., Pulak, R., Ambros, V., and Anderson, P. (1989). A new kind of informational suppression in the nematode *Caenorhabditis elegans*. Genetics *123*, 301–313.

Huntzinger, E., Kashima, I., Fauser, M., Saulière, J., and Izaurralde, E. (2008). SMG6 is the catalytic endonuclease that cleaves mRNAs containing nonsense codons in metazoan. RNA *14*, 2609–2617.

Imamura, K., Maeda, S., Kawamura, I., Matsuyama, K., Shinohara, N., Yahiro, Y., Nagano, S., Setoguchi, T., Yokouchi, M., Ishidou, Y., et al. (2014). Human immunodeficiency virus type 1 enhancer-binding protein 3 is essential for the expression of asparagine-linked glycosylation 2 in the regulation of osteoblast and chondrocyte differentiation. J. Biol. Chem. *289*, 9865–9879.

Kim, Y.K., and Maquat, L.E. (2019). UPFront and center in RNA decay: UPF1 in nonsense-mediated mRNA decay and beyond. RNA *25*, 407–422.

Kurosaki, T., Popp, M.W., and Maquat, L.E. (2019). Quality and quantity control of gene expression by nonsense-mediated mRNA decay. Nat. Rev. Mol. Cell Biol. *20*, 406–420.

Li, S.-T., Lu, T.-T., Xu, X.-X., Ding, Y., Li, Z., Kitajima, T., Dean, N., Wang, N., and Gao, X.-D. (2019). Reconstitution of the lipid-linked oligosaccharide pathway for assembly of high-mannose N-glycans. Nat. Commun. *10*, 1813.

Longman, D., Plasterk, R.H., Johnstone, I.L., and Cáceres, J.F. (2007). Mechanistic insights and identification of two novel factors in the *C. elegans* NMD pathway. Genes Dev. *21*, 1075–1085.

Lykke-Andersen, S., Chen, Y., Ardal, B.R., Lilje, B., Waage, J., Sandelin, A., and Jensen, T.H. (2014). Human nonsense-mediated RNA decay initiates widely by endonucleolysis and targets snoRNA host genes. Genes Dev. *28*, 2498–2517.

Mango, S.E. (2001). Stop making nonSense: the *C. elegans smg* genes. Trends Genet. *17*, 646–653.

Mitrovich, Q.M., and Anderson, P. (2000). Unproductively spliced ribosomal protein mRNAs are natural targets of mRNA surveillance in *C. elegans*. Genes Dev. *14*, 2173–2184.

Page, M.F., Carr, B., Anders, K.R., Grimson, A., and Anderson, P. (1999). SMG-2 is a phosphorylated protein required for mRNA surveillance in *Caenorhabditis elegans* and related to Upf1p of yeast. Mol. Cell. Biol. *19*, 5943–5951.

Rahman, M., and Nasrin, F. (2016). Human disease-causing mutations affecting RNA splicing and NMD. J. Investig. Genomics *3*, 00046.

Rosains, J., and Mango, S.E. (2012). Genetic characterization of *smg-8* mutants reveals no role in *C. elegans* nonsense mediated decay. PLoS One *7*, e49490.

Sakaki, K., Yoshina, S., Shen, X., Han, J., DeSantis, M.R., Xiong, M., Mitani, S., and Kaufman, R.J. (2012). RNA surveillance is required for endoplasmic reticulum homeostasis. Proc. Natl. Acad. Sci. U S A *109*, 8079–8084.

Schmid, M., and Jensen, T.H. (2008). The exosome: a multipurpose RNA-decay machine. Trends Biochem. Sci. *33*, 501–510.

Son, H.G., Seo, M., Ham, S., Hwang, W., Lee, D., An, S.W., Artan, M., Seo, K., Kaletsky, R., Arey, R.N., et al. (2017). RNA surveillance via nonsense-mediated mRNA decay is crucial for longevity in *daf-2*/insulin/IGF-1 mutant *C. elegans*. Nat. Commun. *8*, 14749.

Tabrez, S.S., Sharma, R.D., Jain, V., Siddiqui, A.A., and Mukhopadhyay, A. (2017). Differential alternative splicing coupled to nonsense-mediated decay of mRNA ensures dietary restriction-induced longevity. Nat. Commun. *8*, 306.

Usuki, F., Yamashita, A., and Fujimura, M. (2019). Environmental stresses suppress nonsense-mediated mRNA decay (NMD) and affect cells by stabilizing NMD-targeted gene expression. Sci. Rep. *9*, 1279.

Yamashita, A., Izumi, N., Kashima, I., Ohnishi, T., Saari, B., Katsuhata, Y., Muramatsu, R., Morita, T., Iwamatsu, A., Hachiya, T., et al. (2009). SMG-8 and SMG-9, two novel subunits of the SMG-1 complex, regulate remodeling of the mRNA surveillance complex during nonsense-mediated mRNA decay. Genes Dev. *23*, 1091–1105.

iScience, Volume *23*

Supplemental Information

Caenorhabditis elegans algn-2 Is Critical for Longevity Conferred by Enhanced Nonsense-Mediated mRNA Decay

Eun Ji E. Kim, Heehwa G. Son, Hae-Eun H. Park, Yoonji Jung, Sujeong Kwon, and Seung-Jae V. Lee

Figure S1

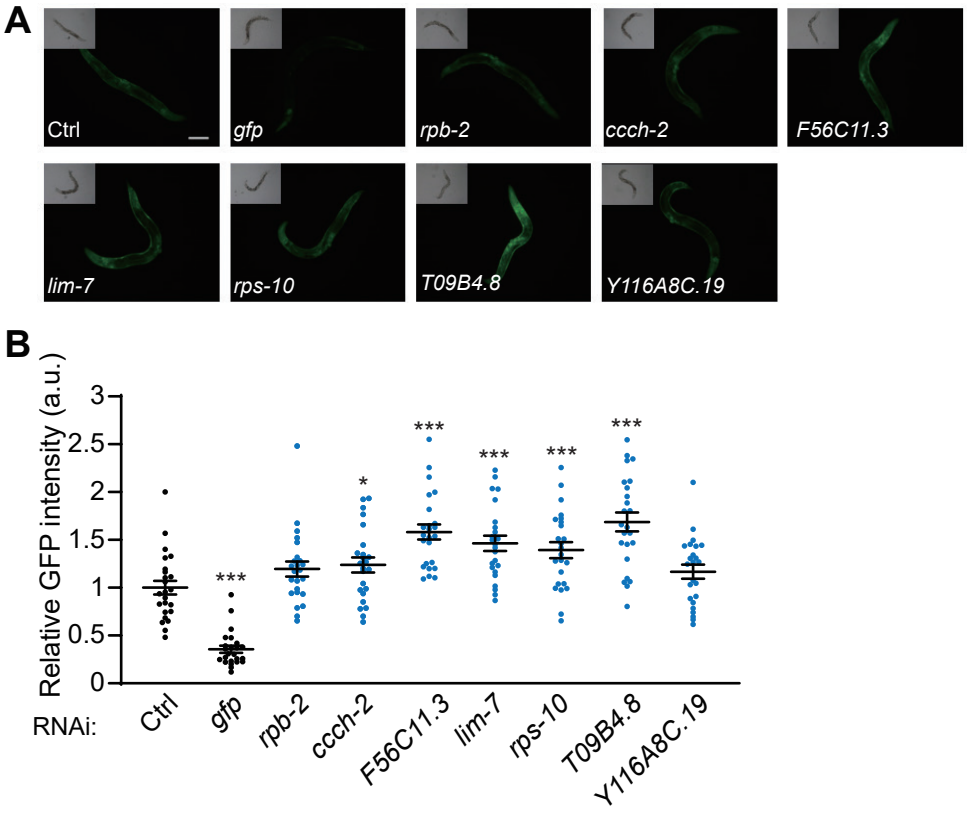
A
Ctrl
gfp
rpb-2
ccch-2
F56C11.3
lim-7
rps-10
T09B4.8
Y116A8C.19
B
Relative GFP intensity (a.u.)
3
2.5
2
1.5
1
0.5
0
***
*
***
***
***
***
RNAi:
Ctrl
gfp
rpb-2
ccch-2
F56C11.3
lim-7
rps-10
T09B4.8
Y116A8C.19

Figure S2

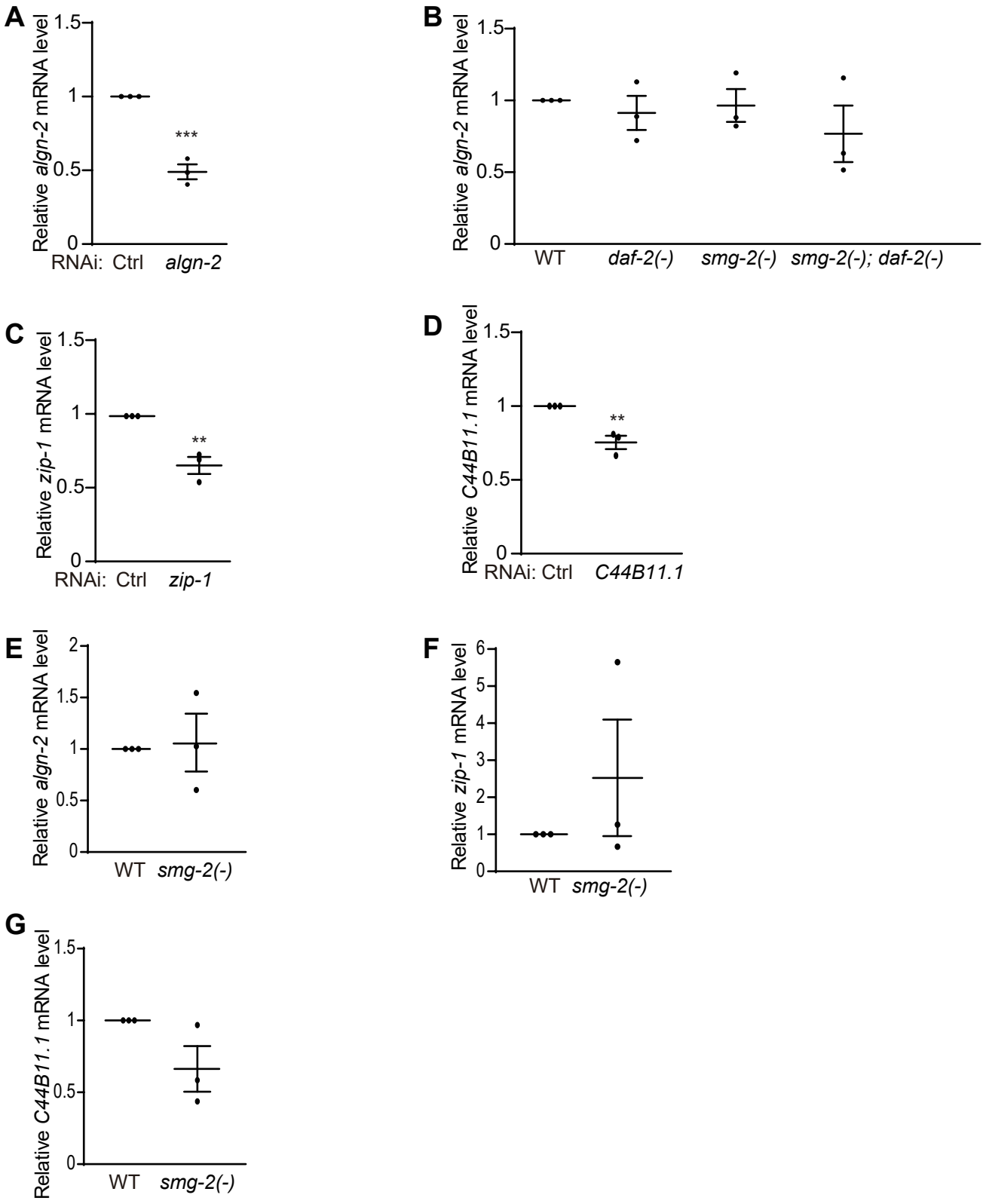
A
Relative algn-2 mRNA level
1.5
1
0.5
0
***
RNAi: Ctrl
algn-2
B
Relative algn-2 mRNA level
1.5
1
0.5
0
WT
daf-2(-)
smg-2(-)
smg-2(-); daf-2(-)
C
Relative zip-1 mRNA level
1.5
1
0.5
0
**
RNAi: Ctrl
zip-1
D
Relative C44B11.1 mRNA level
1.5
1
0.5
0
**
RNAi: Ctrl
C44B11.1
E
Relative algn-2 mRNA level
2
1.5
1
0.5
0
WT
smg-2(-)
F
Relative zip-1 mRNA level
6
5
4
3
2
1
0
WT
smg-2(-)
G
Relative C44B11.1 mRNA level
1.5
1
0.5
0
WT
smg-2(-)

Figure S3

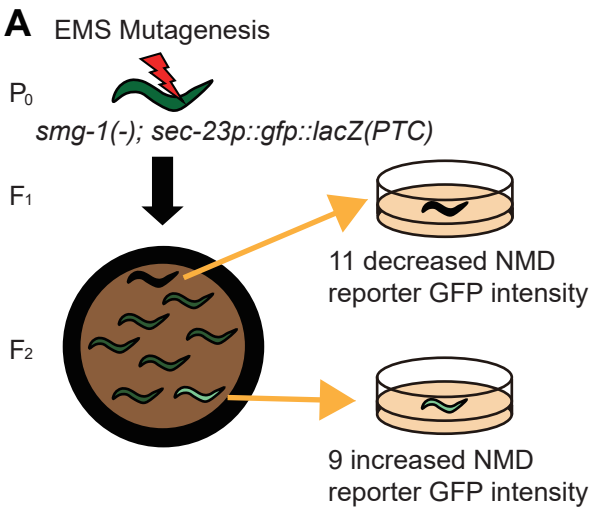
A
EMS Mutagenesis
P0
smg-1(-); sec-23p::gfp::lacZ(PTC)
F1
F2
11 decreased NMD reporter GFP intensity
9 increased NMD reporter GFP intensity

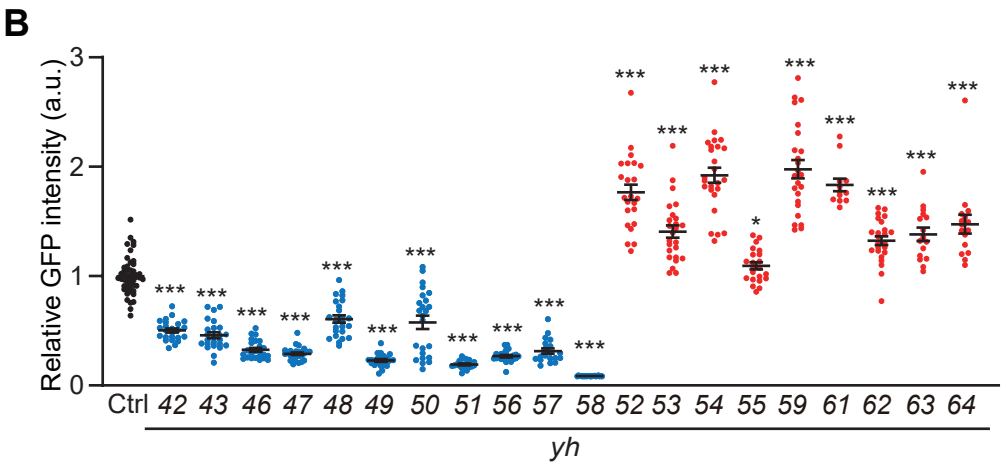
B
Relative GFP intensity (a.u.)
0
1
2
3
Ctrl 42 43 46 47 48 49 50 51 56 57 58 52 53 54 55 59 61 62 63 64
yh

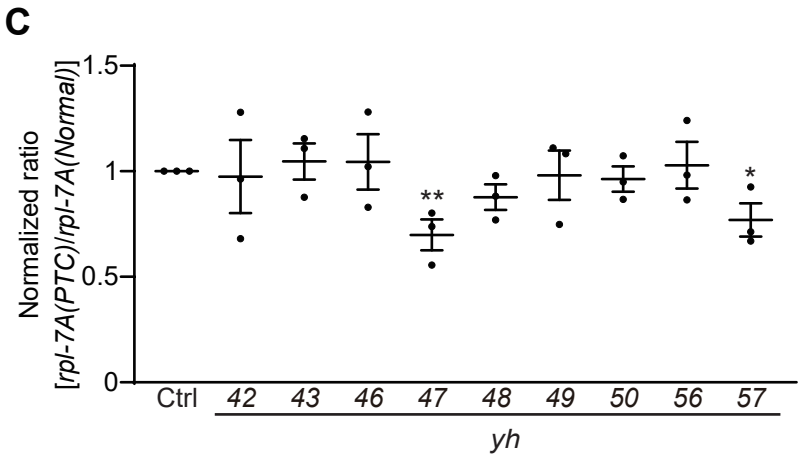
C
Normalized ratio [rpl-7A(PTC)/rpl-7A(Normal)]
0
0.5
1
1.5
Ctrl 42 43 46 47 48 49 50 56 57
yh

Figure S4

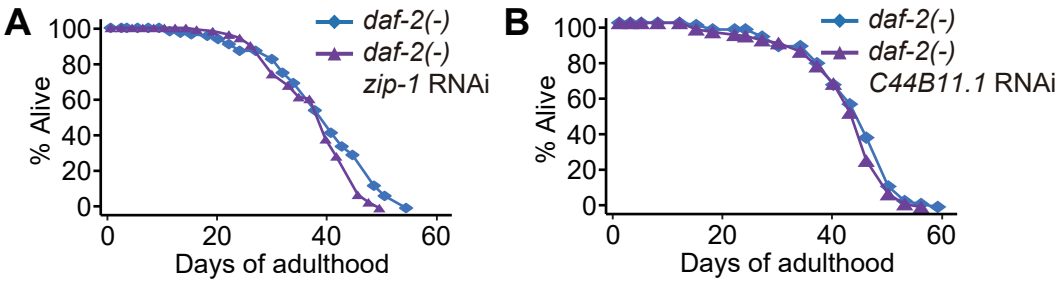
A
100
80
60
40
20
0
% Alive
0
20
40
60
Days of adulthood
daf-2(-)
daf-2(-)
zip-1 RNAi
B
100
80
60
40
20
0
% Alive
0
20
40
60
Days of adulthood
daf-2(-)
daf-2(-)
C44B11.1 RNAi

Figure S5

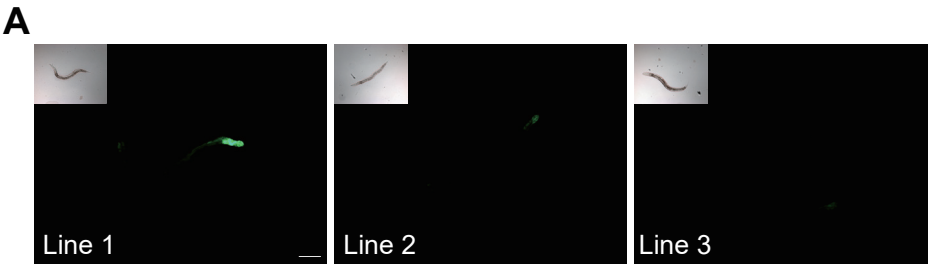
A
Line 1
Line 2
Line 3

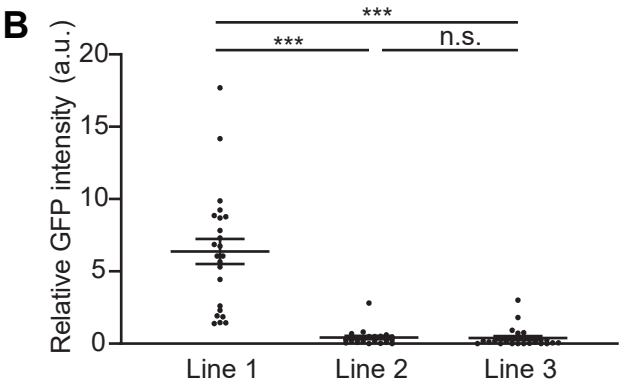
B
***
***
n.s.
Relative GFP intensity (a.u.)
0
5
10
15
20
Line 1
Line 2
Line 3

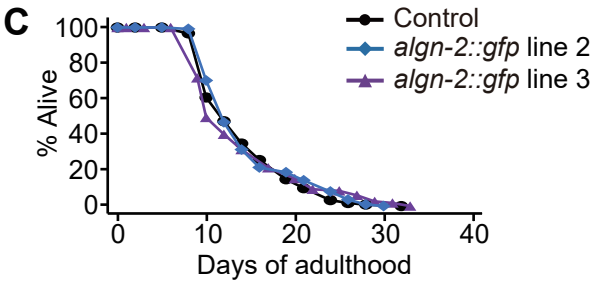
C
Control
algn-2::gfp line 2
algn-2::gfp line 3
% Alive
0
20
40
60
80
100
0
10
20
30
40
Days of adulthood

Supplemental Information

Supplemental Figure Legends

Figure S1. RNAi clones that decreased GFP levels in liquid culture media did not exert similar effects on solid media, related to Figures 1 and 2. (**A**) Seven representative RNAi clones that decreased GFP levels from a genome-wide RNAi screen on solid media (scale bar, 100 μm). *gfp* RNAi was used as a positive control. (**B**) Quantification data of images shown in panel **A**. Some of the hit RNAi clones from our screen may include false positives that affect transgene expression rather than NMD function. RNAi targeting each of *hlh-28*, *K12H6.2*, *ubc-1*, *W10G11.19*, and *rnf-5* that increased the levels of the NMD reporter GFP in this study have been reported to increase the expression of other transgenes (Broday et al., 2004; Kapulkin et al., 2005; Lamitina et al., 2006; Marza et al., 2015; Quach et al., 2013). In addition, *ccch-2* and *rpb-2* RNAi clones that decreased our NMD reporter GFP level have been shown to decrease transgene expression (MacNeil et al., 2015; Winter et al., 2012). Thus, it seems likely that some of our hit RNAi clones altered the GFP levels in the NMD reporter transgenic worms by generally altering transgene expression, independently of NMD function. Therefore, our additional qRT-PCR experiments, which measured endogenous NMD target mRNA levels, validated genuine hit RNAi clones that affected NMD. We also noticed that increases in *rpl-7A(PTC)* mRNA levels caused by RNAi targeting each of *algn-2*, *zip-1*, and *C44B11.1* were smaller than those caused by *smg-2* RNAi (Fig. 2D); this is different from the similar effects of these three RNAi clones and *smg-2* RNAi on the changes in the NMD reporter GFP levels (Fig. 2A-B). SMG-2 is the central component of NMD

(Isken and Maquat, 2008; Kim and Maquat, 2019), and therefore *smg-2* RNAi resulted in a striking increase in *rpl-7A(PTC)* mRNA levels as NMD cannot function properly. In contrast, *algn-2*, *zip-1*, and *C44B11.1* appear to be modulators of NMD. Thus, we speculate that the effects of *algn-2* RNAi, *zip-1* RNAi, and *C44B11.1* RNAi on *rpl-7A(PTC)* mRNA levels are smaller than that of *smg-2* RNAi. Error bars represent s.e.m (two-tailed Student's *t*-test, **p* < 0.05, ****p* < 0.001, n=24 from three independent experiments, a.u.: arbitrary unit). See Supplemental Table S1 for the descriptions and scores of indicated RNAi clones from the screen.

Figure S2. The effects of various genetic interventions that we tested in this study on the mRNA levels of NMD targets and regulators, related to Figures 3 and 4. (**A**) *algn-2* RNAi significantly decreased the mRNA levels of *algn-2* in wild-type worms measured by using qRT-PCR (n=3). (**B**) *algn-2* mRNA levels were similar among wild-type (WT), *daf-2(e1370)* [*daf-2(-)*], *smg-2(qd101)* [*smg-2(-)*], and *smg-2(-); daf-2(-)* mutant animals (n=3). (**C-D**) *zip-1* RNAi (**C**) and *C44B11.1* RNAi (**D**) significantly decreased the mRNA levels of *zip-1* and *C44B11.1*, respectively, in WT worms (n=3). (**E-G**) The mRNA level of *algn-2* (**E**), *zip-1* (**F**), or *C44B11.1* (**G**) was not significantly altered in *smg-2(qd101)* [*smg-2(-)*] mutants compared with that in WT animals (n=3). Error bars represent s.e.m (two-tailed Student's *t*-test, ***p* < 0.01, ****p* < 0.001).

Figure S3. EMS mutagenesis screen for mutants with altered NMD function, related to Figure 2. (**A**) Our EMS mutagenesis screen identified 11 suppressors and

9 enhancers that decreased and increased the GFP intensity, respectively, in *smg-1(-); sec-23p::gfp::lacZ(PTC)* animals. See Supplemental Table S2 for isolated mutants and their lineage. (**B**) Quantification of the GFP fluorescence levels of isolated mutants compared to the control (Ctrl), *smg-1(-); sec-23p::gfp::lacZ(PTC)* animals. a.u.: arbitrary unit. Error bars represent s.e.m (two-tailed Student's *t*-test, **p* < 0.05, ****p* < 0.001, n ≥ 24). (**C**) *rpl-7A(PTC)* levels normalized to *rpl-7A(Normal)* measured by qRT-PCR with mutants that displayed decreased GFP levels from the EMS mutagenesis screen using *smg-1(-); sec-23p::gfp::lacZ(PTC)* animals as a control. Error bars represent s.e.m (two-tailed Student's *t*-test, **p* < 0.05, ***p* < 0.01, n=3).

Figure S4. *zip-1* RNAi or *C44B11.1* RNAi did not affect the lifespan of *daf-2(e1370)* mutants, related to Figure 4. RNAi targeting *zip-1* (**A**) or *C44B11.1* (**B**) did not affect longevity conferred by *daf-2(e1370)* [*daf-2(-)*] mutations. We showed that the mRNA level of *algn-2* positively correlates with NMD function with age (Fig. 3A). In contrast, the mRNA level of *C44B11.1* increased with age but the NMD function decreased with age (Fig. 3C). One can speculate that *C44B11.1* expression increases in an age-dependent manner to compensate the impaired NMD in old worms. *C44B11.1* RNAi did not affect lifespan (Fig. 3F), whereas *algn-2* RNAi significantly shortened lifespan (Fig. 3D). This is likely because *algn-2* affects NMD targets that are critical for lifespan regulation, whereas *C44B11.1* may regulate a different subset of NMD targets that have a small or no effect on lifespan. See Supplemental Table S3 for statistical analysis and additional lifespan data.

Figure S5. Lifespan assay using *algn-2::gfp*, related to Figure 5. (**A**-**B**) The images of three transgenic lines that expressed *algn-2::gfp*. *yhEx540[algn-2p::algn-2::gfp; ofm-1p::rfp]* [Line 1]*, yhEx541[algn-2p::algn-2::gfp; ofm-1p::rfp]* [Line 2], and *yhEx542[algn-2p::algn-2::gfp; ofm-1p::rfp]* [Line 3] (scale bar, 100 μm). (**B**) Quantification of ALGN-2::GFP levels in panel **A**. Error bars represent s.e.m (two-tailed Student's *t*-test, ***$p < 0.001$, n=24 from three independent experiments, a.u.: arbitrary unit.). (**C**) *algn-2::gfp* line 2 or *algn-2::gfp* line 3 did not affect lifespan. See Supplemental Table S3 for statistical analysis and additional lifespan data.

Transparent Methods

Strains

The following strains were used in this study: Lee laboratory N2 wild-type (WT), IJ1600 *smg-1(tm849) I* outcrossed eight times with N2, PTCxi *sec-23p::gfp::lacZ(PTC)*, IJ1601 *smg-1(tm849); sec-23p::gfp::lacZ(PTC)* obtained by crossing FX17751 *smg-1(tm849)* and PTCxi, *sec-23p::gfp::lacZ*, IJ445 *smg-2(qd101)* I outcrossed four times with N2, CF1041 *daf-2(e1370) III* outcrossed six times with N2, IJ446 *smg-2(qd101) I; daf-2(e1370) III*, IJ385 *daf-2(e1368) III* outcrossed nine times with N2, IJ256 *age-1(hx546) II* outcrossed four times with N2, IJ173 *eat-2(ad1116) II* outcrossed four times with N2, CF2172 *isp-1(qm150) IV* outcrossed three times with N2, IJ1754 *smg-1(tm849); sec-23p::gfp::lacZ(PTC); (yh42)* IJ1755 *smg-1(tm849); sec-23p::gfp::lacZ(PTC); (yh43),* IJ1756 *smg-1(tm849); sec-23p::gfp::lacZ(PTC); (yh46)*, IJ1757 *smg-1(tm849); sec-23p::gfp::lacZ(PTC); (yh47)*,

IJ1758 *smg-1(tm849); sec-23p::gfp::lacZ(PTC); (yh48)*, IJ1759 *smg-1(tm849); sec-23p::gfp::lacZ(PTC); (yh49)*, IJ1760 *smg-1(tm849); sec-23p::gfp::lacZ(PTC); (yh50)*, IJ1761 *smg-1(tm849); sec-23p::gfp::lacZ(PTC); (yh51)*, IJ1766 *smg-1(tm849); sec-23p::gfp::lacZ(PTC); (yh56)*, IJ1767 *smg-1(tm849); sec-23p::gfp::lacZ(PTC); (yh57)*, IJ1768 *smg-1(tm849); sec-23p::gfp::lacZ(PTC); (yh58)*, IJ1762 *smg-1(tm849); sec-23p::gfp::lacZ(PTC); (yh52)*, IJ1763 *smg-1(tm849); sec-23p::gfp::lacZ(PTC); (yh53)*, IJ1764 *smg-1(tm849); sec-23p::gfp::lacZ(PTC); (yh54)*, IJ1765 *smg-1(tm849); sec-23p::gfp::lacZ(PTC); (yh55)*, IJ1769 *smg-1(tm849); sec-23p::gfp::lacZ(PTC); (yh59)*, IJ1771 *smg-1(tm849); sec-23p::gfp::lacZ(PTC); (yh61)*, IJ1772 *smg-1(tm849); sec-23p::gfp::lacZ(PTC); (yh62)*, IJ1773 *smg-1(tm849); sec-23p::gfp::lacZ(PTC); (yh63)*, IJ1774 *smg-1(tm849); sec-23p::gfp::lacZ(PTC); (yh64)*, IJ1539 *yhEx414[ofm-1p::rfp]*, IJ2047 *yhEx540[algn-2p::algn-2::gfp; ofm-1p::rfp],* IJ2048 *yhEx541*[*algn-2p::algn-2::gfp; ofm-1p::rfp*], IJ2049 *yhEx542[algn-2p::algn-2::gfp; ofm-1p::rfp]*. All strains were maintained at 20°C.

Genome-wide RNAi screen

A genome-wide RNAi screen was performed based on a previous study (Lee et al., 2010), with some modifications. Gravid adult *smg-1(tm849); sec-23p::gfp::lacZ(PTC)* animals were treated with bleach to obtain eggs (Stiernagle, 2006). The collected eggs were incubated in M9 buffer at 20°C for approximately 18 h. On the same day as worms were bleached, double-stranded (ds) RNA–expressing HT115 bacteria from a commercially available *C. elegans* RNAi library (Source BioScience, Nottingham, UK) were cultured in Luria broth (LB) containing 100 μg/ml ampicillin in

96-well plates overnight at 37°C. On the following day, isopropylthiogalactoside (IPTG) (Gold biotechnology, St Louis, MO, USA) was added to each well of the bacterial cultures to a final concentration of 4 mM, and the plates were placed in a 37°C incubator for 1 h. Bacterial pellets were collected by spinning down at 870 *g* for 10 min. The supernatant was discarded and 190 µl liquid nematode growth media (NGM) containing 100 µg/ml ampicillin plus 4 mM IPTG solution was added to the bacterial pellets. Approximately 20 L1 larval worms were added to each well with cultured bacteria and incubated at 20°C in a shaking incubator. Three days later, the plates were scored for GFP intensity by four researchers independently. Semi-quantitative GFP scores ranging from −3 (darkest) to +3 (brightest) were given to each well. Control empty vector RNAi (L4440) and *gfp* RNAi were used as controls to provide references for scores 0 and −3, respectively. From the primary RNAi screen, arbitrary cutoff scores for positive hits were set (> +1.5 and < −1.5). The liquid-based screen was repeated six times by the four independent researchers using an RNAi sublibrary that included 77 candidate RNAi clones from our initial RNAi screen. The mean scores of the six repeats were calculated and arbitrary cutoff scores were set as the values +0.6 and −0.6.

Microscopy

Fluorescence imaging was performed based on a previous study (Lee et al., 2015), with some modifications. For measuring GFP fluorescence levels in *smg-1(tm849) I; PTCxi::GFP* animals, the transgenic worms were fed with designated RNAi bacteria from hatching. Synchronized young adult (day 0) worms were placed on a 2%

agarose pad and paralyzed with 2 mM levamisole. Images of the worms were captured using an AxioCam HRc CCD digital camera connected to a Zeiss Axio Scope A1 microscope. The fluorescence intensity of the worms was quantified using ImageJ (http://imagesj.nih.gov/ij/) (Schneider et al., 2012) after subtracting background fluorescence signals. Confocal fluorescence images of *algn-2p::algn-2::gfp* worms were acquired using an inverted LSM880 laser scanning microscope (Zeiss Corporation, Germany) with Plan Apochromat 20x0.8 M27, Plan-Apochromat 63x1.4 oil DIC M27 objectives. Green fluorescence was detected with the excitation wavelength at 488 nm and emission wavelength 526 nm.

EMS mutagenesis screen

An EMS mutagenesis screen was performed based on a previous study (Gürel et al., 2012), with some modifications. *smg-1(tm849) I; PTCxi::GFP* transgenic worms (1,150 animals) at the late L4 stage were collected, washed twice with M9 buffer, and placed in 2 ml M9 buffer. The worms were then treated with 47 mM liquid ethyl methanesulfonate (EMS, Sigma, St. Louis, MO, USA) and incubated at 20°C for 4 h with shaking. The worms were then washed twice with M9 buffer and transferred onto OP50-seeded NGM plates to recover for 4 h. The EMS-treated P_0 worms were then evenly transferred onto 14 NGM plates and removed from the plates 24 h later, when F_1 progeny were generated. Gravid 41,700 F_1 adults were then treated with bleach solution to obtain F_2 eggs. Approximately 500 F_2 eggs were placed on each NGM plate (400 plates total) and grown to adulthood. The F_2 adult worms that exhibited greater or lesser GFP intensity than control worms were isolated and individually cultured to establish mutant lines. Initially, 98 mutants (63 with increased

GFP levels and 35 with decreased GFP levels) were isolated. Among these 98 mutant lines, 35 and 15 mutants that exhibited increased and decreased GFP levels, respectively, were sterile; the increased and decreased GFP levels of 19 and 9 mutants, respectively, were not reproducible. Finally, 9 and 11 mutant strains that reproducibly displayed increased and decreased GFP fluorescence, respectively, relative to control RNAi-treated worms were established.

RT-PCR

RT-PCR was performed based on a previous study (Son et al., 2017), with some modifications. dsRNA-expressing HT115 bacteria were cultured in LB containing 50 μg/ml ampicillin overnight at 37°C. The bacteria were then seeded on NGM plates and incubated overnight at 37°C. IPTG (1 mM) was added onto the bacteria-seeded plates, which were then kept at room temperature for 1 d. Approximately 500 bleached eggs of *smg-1(tm849)* mutants were placed on the plates and grown until reaching the young adult stage. Total RNA was extracted from synchronized worms using RNA IsoPlus (Takara, Shiga, Japan). cDNA was generated using ReverTra Ace® qPCR RT Master Mix with gDNA remover (Toyobo, Osaka, Japan). *rpl-7A(PTC)* and *rpl-7A(Normal)* cDNAs were amplified using the primers that were reported (Rosains and Mango, 2012). PCR products were analyzed by electrophoresis on a 2% agarose gel for 25 min. The band intensity was quantified using ImageJ (http://imagesj.nih.gov/ij/). The sequences of the primers that were used are as follows:

rpl-7A(PTC)-F: GACAGCCAGTCCGGTTGG

rpl-7A(PTC)-R: -GTCTAGTTCACCTATCAGAGTAAATG

rpl-7A(Normal)-F: GACATCCAGCCAAAGAAGGA

rpl-7A(Normal)-R: AACGGTGTTTGGTCTCTTGG

Quantitative RT-PCR analysis

Quantitative RT-PCR was performed based on a previous study (Jeong et al., 2020), with some modifications. All worms were maintained at 20°C. Levels of *rpl-7A(PTC)* transcript were measured using the mutant worms that we isolated, and *smg-1(tm849); sec-23p::gfp::lacZ(PTC)* transgenic animals were used as a control. Total RNA was extracted from synchronized day 1 adult worms using RNA IsoPlus. cDNA was generated using ReverTra Ace® qPCR RT Master Mix with gDNA remover and was used for quantitative PCR to measure mRNA levels. Quantitative PCR with the Power SYBR® Green PCR master mix (Applied Biosystems, Foster City, CA, USA) was performed using a StepOne Real Time PCR System (Applied Biosystems, Foster City, CA, USA). The analysis was performed by using a comparative C_T method. The *ama-1* mRNA level was used as a control for normalization. The sequences of the primers that were used are as follows:

ama-1-F: TGGAACTCTGGAGTCACACC

ama-1-R: CATCCTCCTTCATTGAACGG

rpl-7A(PTC)-F: GACAGCCAGTCCGGTTGG

rpl-7A(PTC)-R: GTCTAGTTCACCTATCAGAGTAAATG

rpl-7A(Normal)-F: GACATCCAGCCAAAGAAGGA

rpl-7A(Normal)-R: AACGGTGTTTGGTCTCTTGG

rpl-12(PTC)-F: GTGATTTTCATGCTCCTGAAG

rpl-12(PTC)-R: CAAGGATCTCCTTGACGG

rpl-12(Normal)-F: AGTCAATTCGCCGGCGC

rpl-12(Normal)-R: GGGTCGAACTTTGGTGGC

algn-2-F: CCGGGTAACCATTCTCCATC

algn-2-R: CGAGGACACTCTGTTCGG

zip-1-F: GAAGGATTTTTTGAGCGAAA

zip-1-R: CCATTTTTTTCTCAATTTCTCACC

C44B11.1-F: CATGGAACAACGACTGGGAAG

C44B11.1-R: GCTTCCTTTCCAACCAGCTTAAAC

Lifespan assays

Lifespan assays were performed based on a previous study (Lee et al., 2019), with some modifications. HT115 bacteria that expressed dsRNA were cultured in LB containing 50 μg/ml ampicillin (USB, Santa Clara, CA, USA) at 37°C overnight. The cultured HT115 RNAi bacteria (100 μl) were then seeded on NGM containing 50 μg/ml ampicillin and incubated at 37°C overnight. IPTG (1 mM) was added and incubated for 24 h at room temperature. To prevent progeny from hatching, 5-fluoro-

2’-deoxyuridine (FUDR) was added to the RNAi bacteria-seeded plates at a final concentration of 5 μM. Young (day 1) adult worms were placed on freshly prepared plates and subsequently transferred onto new plates after 1 or 2 d. Worms that did not respond to a gentle touch with a platinum wire pick were scored as dead. Worms that ruptured, burrowed, bagged, or crawled off the plates were censored but included for subsequent statistical analysis. All lifespan assays were performed at 20°C by at least two independent researchers. OASIS (online application of survival analysis, http://sbi.postech.ac.kr/oasis) was used for statistical analysis of the lifespan assay results (Yang et al., 2011). A log-rank (Mantel-Cox method) test was used to calculate *p* values.

Cloning and generation of transgenic worms

A promoter (~0.3 kb upstream of the start codon) and the coding region of *algn-2* (~1.8 kb) were PCR amplified by using *C. elegans* genomic DNA as a PCR template. pPD95.75 (Fire lab *C. elegans* vector kit) plasmid was linearized by KpnI restriction enzyme. The PCR product of *algn-2* promoter and *algn-2* genomic region were inserted into the linearized pPD95.75 using In-fusion HD cloning kit (Takara, Shiga, Japan) to generate *algn-2p::algn-2::gfp* plasmid. The mixture of *algn-2p::algn-2::gfp* plasmid (25 ng μl^{-1}) and the control plasmid *ofm-1p::rfp* (75 ng μl^{-1}) were injected into day 1 adult worms.

Supplemental References

Broday, L., Kolotuev, I., Didier, C., Bhoumik, A., Podbilewicz, B., and Ronai, Z. (2004). The LIM domain protein UNC-95 is required for the assembly of muscle attachment structures and is regulated by the RING finger protein RNF-5 in *C. elegans*. J Cell Biol *165*, 857-867.

Gürel, G., Gustafson, M.A., Pepper, J.S., Horvitz, H.R., and Koelle, M.R. (2012). Receptors and other signaling proteins required for serotonin control of locomotion in *Caenorhabditis elegans*. Genetics *192*, 1359-1371.

Isken, O., and Maquat, L.E. (2008). The multiple lives of NMD factors: balancing roles in gene and genome regulation. Nature reviews. Genetics *9*, 699-712.

Jeong, D.E., Lee, Y., Ham, S., Lee, D., Kwon, S., Park, H.H., Hwang, S.Y., Yoo, J.Y., Roh, T.Y., and Lee, S.V. (2020). Inhibition of the oligosaccharyl transferase in *Caenorhabditis elegans* that compromises ER proteostasis suppresses p38-dependent protection against pathogenic bacteria. PLoS genetics *16*, e1008617.

Kapulkin, W.J., Hiester, B.G., and Link, C.D. (2005). Compensatory regulation among ER chaperones in *C. elegans*. FEBS Lett *579*, 3063-3068.

Kim, Y.K., and Maquat, L.E. (2019). UPFront and center in RNA decay: UPF1 in nonsense-mediated mRNA decay and beyond. RNA (New York, N.Y.) *25*, 407-422.

Lamitina, T., Huang, C.G., and Strange, K. (2006). Genome-wide RNAi screening identifies protein damage as a regulator of osmoprotective gene expression. Proc Natl Acad Sci U S A *103*, 12173-12178.

Lee, D., An, S.W.A., Jung, Y., Yamaoka, Y., Ryu, Y., Goh, G.Y.S., Beigi, A., Yang, J.-S., Jung, G.Y., Ma, D.K.*, et al.* (2019). MDT-15/MED15 permits longevity at low temperature via enhancing lipidostasis and proteostasis. PLOS Biology *17*, e3000415.

Lee, D., Jeong, D.E., Son, H.G., Yamaoka, Y., Kim, H., Seo, K., Khan, A.A., Roh, T.Y., Moon, D.W., Lee, Y.*, et al.* (2015). SREBP and MDT-15 protect *C. elegans* from glucose-induced accelerated aging by preventing accumulation of saturated fat. Genes Dev *29*, 2490-2503.

Lee, S.J., Hwang, A.B., and Kenyon, C. (2010). Inhibition of respiration extends *C. elegans* life span via reactive oxygen species that increase HIF-1 activity. Current biology : CB *20*, 2131-2136.

MacNeil, L.T., Pons, C., Arda, H.E., Giese, G.E., Myers, C.L., and Walhout, A.J. (2015). Transcription Factor Activity Mapping of a Tissue-Specific in vivo Gene Regulatory Network. Cell systems *1*, 152-162.

Marza, E., Taouji, S., Barroso, K., Raymond, A.A., Guignard, L., Bonneu, M., Pallares-Lupon, N., Dupuy, J.W., Fernandez-Zapico, M.E., Rosenbaum, J.*, et al.* (2015). Genome-wide screen identifies a novel p97/CDC-48-dependent pathway regulating ER-stress-induced gene transcription. EMBO reports *16*, 332-340.

Quach, T.K., Chou, H.T., Wang, K., Milledge, G.Z., and Johnson, C.M. (2013). Genome-wide microarrray analysis reveals roles for the REF-1 family member HLH-29 in ferritin synthesis and peroxide stress response. PLoS One *8*, e59719.

Schneider, C.A., Rasband, W.S., and Eliceiri, K.W. (2012). NIH Image to ImageJ: 25 years of image analysis. Nature methods *9*, 671-675.

Son, H.G., Seo, M., Ham, S., Hwang, W., Lee, D., An, S.W., Artan, M., Seo, K., Kaletsky, R., Arey, R.N.*, et al.* (2017). RNA surveillance via nonsense-mediated mRNA decay is crucial for longevity in *daf-2*/insulin/IGF-1 mutant *C. elegans*. Nat Commun *8*, 14749.

Stiernagle, T. (2006). Maintenance of *C. elegans*. WormBook : the online review of

C. elegans biology, 1-11.

Winter, J.F., Höpfner, S., Korn, K., Farnung, B.O., Bradshaw, C.R., Marsico, G., Volkmer, M., Habermann, B., and Zerial, M. (2012). *Caenorhabditis elegans* screen reveals role of PAR-5 in RAB-11-recycling endosome positioning and apicobasal cell polarity. Nature cell biology *14*, 666-676.

Yang, J.S., Nam, H.J., Seo, M., Han, S.K., Choi, Y., Nam, H.G., Lee, S.J., and Kim, S. (2011). OASIS: online application for the survival analysis of lifespan assays performed in aging research. PLoS One *6*, e23525.